Received: 18 March 2026 | **Revised:** 01 April 2026 | **Accepted:** 10 April 2026 Science Research Annals—Physical Sciences 2(1), 13–21

SCIENCE RESEARCH ANNALS
(PHYSICAL SCIENCES)

Published by the Faculty of Science, Adekunle Ajasin University, Akungba-Akoko (AAUA)

Journal website: https://sra.com.ng/index.php/sra-physical

SCIENTIFIC ARTICLE DOI: https://doi.org/10.63112/zys4jd37

Effects of viscous dissipation and micropolar heat conduction on thermally radiating MHD flow along a vertical plate

Adetunji Adeniyan [1,*], Ephesus O. Fatunmbi [2]

[1] *Department of Mathematics, Trinity University, Yaba, Lagos State, Nigeria*
[2] *Department of Mathematics and Statistics, Federal Polytechnic Ilaro, PMB 50, Ilaro, Ogun State, Nigeria*

*Correspondence: tunjiadeniyan@yahoo.com; professorsoji@gmail.com (A. Adeniyan)

ARTICLE INFORMATION

Keywords:
Viscous dissipation
Micropolar fluid
Heat conduction
Thermal radiation
Magnetohydrodynamics

Handling Editor: A. S. Oke

ABSTRACT

This study investigates the combined effects of viscous dissipation and micropolar heat conduction on steady magnetohydrodynamic (MHD) flow of a thermally radiating micropolar fluid along a vertical plate. The governing nonlinear partial differential equations describing momentum, microrotation, and energy transport are formulated by incorporating Joule heating, viscous dissipation, and Rosseland thermal radiation. Using appropriate similarity transformations, the system is reduced to a set of coupled ordinary differential equations and solved numerically by the shooting method alongside the Runge-Kutta-Fehlberg scheme. The influences of key dimensionless parameters, including the magnetic parameter, Eckert number, micropolar material parameter, radiation parameter, and Prandtl number, on velocity, microrotation, and temperature distributions are analyzed in detail. The results reveal that viscous dissipation significantly increases fluid temperature and the thickness of the thermal boundary layer, while enhanced micropolar heat conduction improves thermal diffusion and modifies microrotation behavior. The applied magnetic field suppresses fluid motion due to Lorentz forces but increases thermal energy through Joule heating. Furthermore, variations in radiation intensity significantly influence the heat transfer rate. A rise in the fluid material term decreases the skin friction coefficient by 17.5%. This reduction is attributed to the enhanced microstructure effects, which allow rotation of fluid particles and reduce shear stress. These findings provide useful insights for optimizing thermal management in practical systems such as MHD pumps, nuclear reactor cooling systems, metallurgical processing units, and solar thermal energy devices.

Highlights

- Micropolar heat conduction reduces temperature and cools the surface
- Higher velocity ratio speeds flow, thins thermal and spin layers.
- Magnetic field slows velocity but raises temperature via Joule heating.
- Stronger radiation expands thermal layer and increases temperature.
- Radiation and viscous dissipation both act as internal heat sources.

1. Introduction

Fluid flow and heat transfer processes involving complex fluids, particularly non-Newtonian fluids, have attracted considerable attention due to their wide range of engineering and industrial applications. Classical Newtonian fluid models are often insufficient to describe fluids possessing microstructure, such as polymeric suspensions, liquid crystals, blood, lubricants, and colloidal fluids (Garg et al., 2025; Fatunmbi & Okoya, 2020; Wu & Massoudi, 2020). To overcome these limitations, the theory of micropolar fluids was introduced by Eringen (1966). This model incorporates the microrotation and micro-inertia of fluid particles and extends the classical Navier–Stokes equations by allowing fluid particles to undergo both translational and rotational motions. Consequently, micropolar fluid theory provides a more realistic representation of many complex fluids encountered in engineering and biological systems (Abbas et al., 2022; Arifuzzaman et al., 2028). Due to these unique characteristics and practical importance, many researchers have studied this fluid model in detail. For instance, Łukaszewicz (1999) presented comprehensive theoretical and practical applications of micropolar fluids, whereas Milan Kocić et al. (2023) investigated

magnetohydrodynamic (MHD) micropolar fluid flow through porous media under the influence of a magnetic field. Fatunmbi and Adeniyan (2018) also examined heat and mass transfer characteristics in MHD micropolar fluids flowing over a stretching sheet with slip effects, while Khan et al. (2020) assessed the flow dynamics of such a fluid model with temperature-dependent transport properties. Moreover, Pasha et al. (2022) also focused on generating numerical solutions for micropolar fluids flowing through porous plates with heat transfer influence, while entropy generation in magneto-micropolar fluids flowing through nonlinear porous media was discussed by Fatunmbi and Salawu (2020). These studies revealed the important role of magnetic and thermal properties in the behaviour of micropolar fluids across different configurations.

Although the micropolar fluid theory is effective in capturing the behaviour of complex fluids in many industrial applications, as stated above, fluids that are also electrically conducting in nature are subjected to a magnetic field influence. Fluids' interaction with a magnetic field leads to the MHD effect in the fluids. The presence of a magnetic field affects the flow behaviour of the fluids due to the action of the Lorentz force, which resists the motion of the fluids. This phenomenon is extremely important in many industrial applications. Such a phenomenon affects the momentum and thermal boundary layers in the fluids. Recent studies have examined such a problem, the characteristics of MHD micropolar fluids under different boundary and thermal conditions. Sharma et al. (2023) studied the MHD micropolar fluid flow over a stretching surface with melting and slip effects. Fatunmbi al. (2020) analyzed MHD micropolar flow in porous media with multiple slip conditions, highlighting the combined effects of magnetic forces, porosity, and slip on the flow and heat transfer mechanisms. These studies demonstrate the significant impact of magnetic fields and boundary conditions on MHD micropolar fluid behaviour. However, in addition to magnetic effects, there are other important factors that influence the thermal characteristics of micropolar fluid flow, which are crucial in real-life and engineering applications.

One such significant mechanism that plays a significant role in the process of heat transfer in fluid flow is viscous dissipation, which is defined as the conversion of kinetic energy into internal energy due to viscous effects in the flow fluids (Hayat et al., 2026 & Saleem et al., 2020). This mechanism is more significant in fluids that have high velocities and are more viscous in nature. Saraswathy et al. (2023) observed that when there is a rise in viscous dissipation in fluids, there is a corresponding increase in the temperature of the fluids and the thermal boundary layer. Kataria et al. (2022) studied MHD micropolar flow with nonlinear thermal radiation and observed that due to viscous dissipation in fluids, there is a rise in temperature and a significant effect on thermal boundary layers in fluids. Kumar et al. (2020) studied MHD micropolar flow over a slendering stretching surface with a modified heat flux model and observed that viscous dissipation increases the temperature distribution in fluids. Even though viscous dissipation is found to have a considerable impact on altering thermal transport, there is always a coupling between various heat transfer mechanisms, particularly thermal radiation, especially in high-temperature environments. Thermal radiation is found to be one of the prominent heat transfer modes, especially in engineering devices that operate at high temperatures, such as gas turbines, combustion chambers, solar devices, space technology, etc. (Jin & Tian, 2022; Li et al., 2023; Fatunmbi et al., 2024). Previous studies have shown that thermal radiation is found to increase the thermal energy within the boundary layer, which may enhance or reduce heat transfer depending on the flow characteristics (Reddy & Lakshmi, 2014). These findings notwithstanding, the thermal characteristics of micropolar fluid do not depend only on thermal radiation and viscous dissipation, but there is always a contribution from fluid microstructure.

In micropolar fluid flows, the role of micropolar heat conduction and material parameters is significant in the overall transport characteristics of the fluids. These parameters control the coupling between microrotation and linear momentum and thus affect the velocity, microrotation, and temperature profiles in the boundary layer. The presence of microstructure in fluids increases the heat diffusion rate compared to classical fluids. This is another important feature of micropolar fluids that makes them important in applications such as polymer processing, lubrication systems, microfluidics, and biomedicine (Eringen, 1972; Łukaszewicz, 1999). However, most studies in the literature have studied most of the parameters discussed above in individual cases or in a few combinations without considering the heat conduction coefficient of the micropolar fluid. The combined effect of viscous dissipation and micropolar heat conduction in a thermally radiating MHD micropolar fluid flow over a vertical plate has not been studied much in the literature.

Motivated by existing gaps in the coupled analysis of micropolar transport phenomena under multiple thermal effects, this study examines the steady MHD flow of a micropolar fluid over a vertical plate. The analysis is based on the assumptions of laminar, incompressible, and electrically conducting flow, with negligible induced magnetic field and constant thermophysical properties, while viscous dissipation, thermal radiation, and micropolar heat conduction are retained. The novelty of this work lies in the simultaneous incorporation of viscous dissipation, micropolar heat conduction, and radiative heat transfer within a unified MHD micropolar framework, which has received limited attention in previous studies. Accordingly, the study addresses the following research questions: (i) How do viscous dissipation and thermal radiation jointly influence heat transfer characteristics? (ii) What is the role of micropolar parameters on microrotation and velocity fields under magnetic effects? (iii) How does the magnetic field interact with thermal mechanisms to affect overall energy transport? The governing nonlinear equations for momentum, microrotation, and energy are reduced to ordinary differential equations using similarity transformations and solved numerically. The results provide targeted insights for enhancing thermal management and energy efficiency in systems such as MHD pumps, polymer processing, and high-temperature thermal devices.

2. Problem Formulation and Analysis

Consider a steady two-dimensional incompressible free stream of uniform velocity U_∞, moving over a stationary impervious semi-infinite vertical plate dwelling in an electrically conducting micropolar liquid as depicted in Figure 1. The orientation of the magnetic field is normal to the plate being heated continuously with constant wall temperature T_w. It is assumed that the flow is laminar and that the magnetic Reynolds number is small. Further, the physical properties of the fluid are considered to be non-varying with respect to space and temperature, except for the buoyancy term in the linear momentum equation, where the Boussinesq approximation is applied, and the thermal conductivity in the energy field. An externally applied magnetic field is imposed normal to the flow direction as described in Figure 1. The impact of viscous dissipation, thermal radiation, and micropolar heat conduction is taken into consideration in the heat equation. The vertical plate configuration

is physically realistic and widely used to model heat transfer processes in engineering applications such as cooling of electronic equipment, nuclear reactor walls, metallurgical processes, and MHD energy systems, where buoyancy-driven flow along heated surfaces is common.

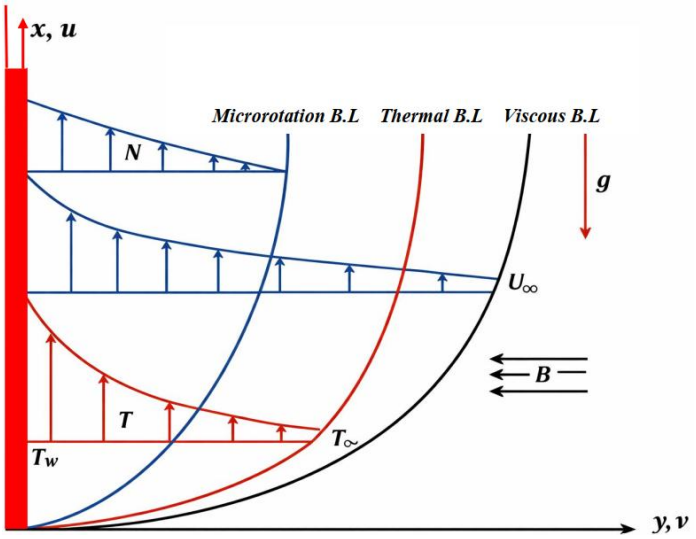

Figure 1: Flow configuration and coordinate system.

Incorporating the above-highlighted assumptions, the relevant governing equations for the momentum, microrotation, energy, and concentration equations are expressed as follows (Bejawada & Nandeppanavar, 2023; Hsiao, 2017).

$$\frac{\partial u}{\partial x}+\frac{\partial v}{\partial y}=0, \tag{1}$$

$$u\frac{\partial u}{\partial x}+v\frac{\partial u}{\partial y}=\frac{\mu+\kappa}{\rho}\frac{\partial^2 u}{\partial y^2}+\frac{\kappa}{\rho}\frac{\partial N}{\partial y}+\frac{\sigma_e B^2(x)}{\rho}(U-u)+g\beta_T(T-T_\infty) \tag{2}$$

$$\rho j\left(u\frac{\partial N}{\partial x}+v\frac{\partial N}{\partial y}\right)=\gamma\frac{\partial^2 N}{\partial y^2}-\kappa\left(2N+\frac{\partial u}{\partial y}\right) \tag{3}$$

$$\rho C_p\left(u\frac{\partial T}{\partial x}+v\frac{\partial T}{\partial y}\right)=\frac{\partial}{\partial y}\left(k(T)\frac{\partial T}{\partial y}\right)+\kappa\left(\frac{\partial u}{\partial y}+N\right)^2-\varepsilon\sigma^*\frac{\partial}{\partial y}(T^4)+q_{iv} \tag{4}$$

where u and v are velocity components in x and y directions, N is the microrotation component, T is the temperature, j is the micro inertial density, μ is the dynamic viscosity, κ is the vortex viscosity, σ_e is the electrical conductivity, ρ describes the density of the fluid, k represents the thermal conductivity. Equation (4) incorporates the approximate radiation heat flux as derived by Cheng (1964). Cheng's thermal radiation model applies to steady or time-dependent situations. In the governing equations, g is gravity acceleration, μ, represents the dynamic viscosity, σ_e represents electrical conductivity, $B(x)=B_0x^{\omega/2}$ is the variable magnetic field, where B_0 is a constant, and ω is the magnetic field variation exponent. In order that the magnetic parameter M be non-local, as given by See Rahman (2009):

$$\frac{\omega+1}{2}=0 \Rightarrow \omega=-1$$

Also, $q_{iv}=\lambda\left(\frac{\partial T}{\partial x}\frac{\partial N}{\partial y}-\frac{\partial T}{\partial y}\frac{\partial N}{\partial x}\right)$ is the micropolar heat conduction, σ^* symbolizes the Stefan-Boltzmann constant, c_p defines the specific heat at constant pressure, q_{iv} and λ is the micropolar heat conduction coefficient. The magnetic field vector and microrotation vector field are respectively defined as $\mathbf{B}=(0,B(x),0)$, $\mathbf{N}=(0,0,N(x,y))$, where $N(x,y)$ represents the microrotation component.

It is assumed that the temperature-dependent thermal conductivity for dilute gases follows the Maxwell power-law relation:

$$k(T)=k_\infty\left(\frac{T}{T_\infty}\right)^n=k_\infty(1+\theta)^n \tag{5}$$

The microrotation viscosity or spin-gradient viscosity γ, as established by Ahmadi (1976), is:

$$\gamma=\left(\mu+\frac{\kappa}{2}\right)j=\mu\left(1+\frac{K}{2}\right)j, \tag{6}$$

The boundary conditions for the present flow problem are expressed as:

$$u=0,v=0,N=-p\left(\frac{\partial u}{\partial y}\right),-k\frac{\partial T}{\partial y}=q_w \text{ at } y=0, \tag{7}$$

$$u\to U_e,N\to 0,T\to T_\infty \text{ as } y\to\infty.$$

Non-dimensional equations:

$$M\eta=y\left(\frac{U_\infty}{\vartheta x}\right)^{0.5},\psi=(\vartheta U_\infty x)^{0.5}f(\eta),N=g(\eta)\left(\frac{U_\infty}{\vartheta x}\right)^{0.5},\theta(\eta)=\frac{T-T_\infty}{T_w-T_\infty},U=\frac{\partial\psi}{\partial y},v=-\frac{\partial\psi}{\partial x} \tag{8}$$

With these, Equation (1) is identically satisfied, indicating that u and v represent the possible components of the fluid velocity. The following equations are obtained from the controlling equations after using (8).

Linear momentum equation:

$$(1+K)f'''+ff''-(f')^2+Kg'+Gr\,\theta-Mf'-\beta f'=0 \tag{9}$$

Angular momentum equation:

$$\left(1+\frac{K}{2}\right)g''+fg'-f'g-K(2g+f'')=0 \tag{10}$$

Energy equation:

$$\frac{1}{Pr}[\theta''+n\theta_R(1+\theta_R\theta)^{-1}\theta^2]+f\theta'-(2\lambda+1)\theta f'+(1+K)Ec(f'')^2-R(1+\theta_R\theta)^4+\alpha[(2\lambda+1)\theta h'-h\theta]=0 \tag{11}$$

Boundary conditions:

$$\eta=0: f(0)=0,f'(0)=0,g(0)=-bf''(0),\theta(0)=1, \tag{12}$$

$\eta \to \infty: f'(\eta) \to \beta, g(\eta) \to 0, \theta(\eta) \to 0$

In the nonlinear coupled ODEs (9–12):

$$M = \frac{\sigma B_0^2}{\rho}, K = \frac{\kappa}{\mu}, \lambda = \frac{\lambda U_0}{\alpha C_p x}, \theta = \frac{T - T_\infty}{\Delta T}, R = \frac{4\varepsilon\sigma^* T_\infty^3 x}{kU}, Ec = \frac{U^2}{C_p \Delta T}, \theta_R, Pr = \frac{\mu c_p}{k} \quad (13)$$

In Equation (13), K is the material parameter, and M is the magnetic parameter, Ec is the Eckert number, θ_R is the thermal conductivity variable term, Pr is the Prandtl number, Ec is the Eckert number, Gr is the Grashof number, β represents the velocity ratio parameter. It is noted that the formulation reduces to the expression in {Takhar, et al., 1998} when $\lambda + 2 = 0$, which corresponds to a special case of the present study. Furthermore, the energy equation simplifies to the classical form in the absence of micropolar heat conduction (i.e., $\lambda = 0$), indicating that the micropolar heat conduction term vanishes. The micropolar heat conducting parameter, relative temperature difference parameter, and the local thermal radiation parameter are given respectively by:

$$\lambda^* = \frac{\lambda U_0}{\alpha C_p x}, \theta = \frac{T - T_\infty}{\Delta T}, R = \frac{4\varepsilon\sigma^* T_\infty^3 x}{kU}, \quad (14)$$

where $\Delta T = T_w - T_\infty$.

Wall shear stress and skin friction:

The wall shear stress is defined as

$$\tau_w = (\mu + \kappa)\frac{\partial u}{\partial y}\Big|_{y=0} + \kappa N(0), \quad (15)$$

The skin friction coefficient is:

$$C_f = \frac{2\tau_w}{\rho U^2}, \quad (16)$$

which leads to:

$$C_f Re_x^{1/2} = (1 + K)[1 - b]f''(0) \quad (17)$$

Wall couple stress:

The wall couple stress is defined as:

$$M_w = \gamma \frac{\partial N}{\partial y}\Big|_{y=0}, \quad (18)$$

and the wall couple stress coefficient becomes:

$$C_s = \left(1 + \frac{K}{2}\right)h'(0) \quad (19)$$

Heat transfer rate:

The heat transfer rate at the wall is given by:

$$q_w = -k\frac{\partial T}{\partial y}\Big|_{y=0}, \quad (20)$$

and including radiation,

$$q_w = -k\frac{\partial T}{\partial y}\Big|_{y=0} - \varepsilon\sigma^*(T_w^4 - T_\infty^4) \quad (21)$$

The local Nusselt number is defined as:

$$Nu_x = \frac{x q_w}{k\Delta T}, \quad (22)$$

Which yields:

$$Nu_x Re_x^{-1/2} = -(1 + \theta)^n \theta'(0) \quad (23)$$

3. Method of Solution

A numerical method has been sought to secure the required solution to the system of equations (9-11) due to the strong nonlinearity of the equations. Thus, the nonlinear BVP. Equations 9–11, alongside the boundary conditions (12), is solved numerically using the shooting technique cum the Runge–Kutta–Fehlberg (RKF45) method. To implement the shooting method, the higher-order differential equations are reduced to a system of first order ordinary diff erential equations by letting:

$$f_1 = f, f_2 = f', f_3 = f'',$$
$$f_4 = h, f_5 = h',$$
$$f_6 = \theta, f_7 = \theta'.$$

In view of this, the governing equations are transformed to:

$$f_1' = f_2,$$
$$f_2' = f_3,$$
$$f_3' = \frac{1}{1+K}[-f_1 f_3 + f_2^2 - K f_5 - Gr f_6 + (M + \beta) f_2],$$
$$f_4' = f_5,$$
$$f_5' = \frac{1}{1 + \frac{K}{2}}[-f_1 f_5 + f_2 f_4 + K(2f_4 + f_3)],$$
$$f_6' = f_7,$$
$$f_7' = \Pr[-f_1 f_7 + (2\lambda + 1) f_6 f_2 - (1 + K) Ec f_3^2 + R\big(1 + \theta_R f_6\big)^4 - \alpha\big((2\lambda + 1) f_6 f_5 - f_4 f_7\big)\big] - n\theta_R (1 + \theta_R f_6)^{-1} f_7^2.$$

Similarly, the wall conditions become:

$$f_1(0) = 0, f_2(0) = 0, f_4(0) = -b f_3(0), f_6(0) = 1$$

Meanwhile, the unknown initial points: $f_3(0) = b_1, f_5(0) = b_2, f_7(0) = b_3$ are calculated iteratively and adjusted such that the BVP is converted into an IVP by guessing the missing initial conditions b_1, b_2, b_3. The system is then integrated from $\eta = 0$ to a sufficiently large finite value η_∞ using the RKF45 method. This continues until the far-field boundary conditions are satisfied, i. e., $f_2(\eta_\infty) \to \beta, f_4(\eta_\infty) \to 0, f_6(\eta_\infty) \to 0$. The RKF45 scheme is employed due to its adaptive step-size control and high accuracy. At each

integration step, both fourth- and fifth-order solutions are computed, and the local truncation error is estimated to adjust the step size dynamically. The iterative procedure is continued until the following convergence criterion is satisfied: $\max\{|f_2(\eta_\infty)-\beta|, |f_4(\eta_\infty)|, |f_6(\eta_\infty)|\} < 10^{-6}$. A finite boundary η_∞ (typically between 8 and 12) is chosen such that the asymptotic boundary conditions are adequately satisfied. To authenticate the accuracy of the numerical scheme, the obtained results are compared with previously published results of Cortell (2005) under limiting cases $(M = K, Ec = Gr = 0)$, showing excellent agreement. As presented in Table 1.

Table 1: Computed values of $f(\eta).f'(\eta)$ and $f''(\eta)$ for variation in η as compared with published work when $\beta = 1$, other parameters are zero.

	Cortell (2005)			Present Results		
η	f	f'	f''	f	f'	f''
0.0	0.00000	0.00000	0.46960	0.00000	0.00000	0.469600
1	0.23299	0.46063	0.43438	0.232990	0.460633	0.434379
2	0.88681	0.81670	0.25567	0.886797	0.816895	0.255669
3	1.79558	0.96906	0.06771	1.783887	0.969065	0.067710
4	2.78300	0.99777	0.00687	2.78300	0.997770	0.006874
5	3.78325	0.99994	0.00026	3.78335	0.999936	0.000258
6	4.78324	1.00000	0.00000	4.783220	0.999999	0.000000

4. Results and Discussion

For a proper understanding of the fluid flow behaviour, a computational analysis is performed to examine the dimensionless velocity, temperature, and microrotation profiles within the boundary layer. The results are presented in both graphical and tabular forms. Table 2 illustrates the effects of the material (micropolar) parameter K, velocity ratio parameter β, and micropolar heat conduction parameter λ, magnetic field parameter M, and Eckert number Ec on the skin friction coefficient C_f, local Nusselt number Nu_x (rate of heat transfer), and the wall couple stress coefficient C_s.

It is observed that the skin friction coefficient C_f increases with increasing values of M, α, and β. Physically, the increase in M strengthens the Lorentz force, which opposes the fluid motion and enhances momentum resistance, thereby increasing shear stress at the wall. Similarly, the parameters α and β contribute to additional resistance within the flow system. In contrast, C_f decreases with increasing K, λ, and Ec. Specifically, a rise in K from 1.0 to 5.0 decreases C_f by 17.5%. The reduction due to K is attributed to the enhanced microstructure effects, which allow rotation of fluid particles and reduce shear stress. Increasing λ enhances thermal diffusion, indirectly reducing viscosity effects, while higher Ec signifies stronger viscous dissipation, which weakens the velocity gradients near the wall.

The rate of heat transfer, represented by Nu_x, decreases with increasing M and Ec. This behaviour is due to the magnetic field suppressing fluid motion, thereby reducing convective heat transfer, while higher viscous dissipation (Ec) increases thermal energy within the fluid, thickening the thermal boundary layer. Conversely, Nu_x increases with increasing values of K, β, and α, which enhance energy transport within the fluid and improve thermal gradients at the wall.

Furthermore, the wall couple stress coefficient C_s decreases with increasing β and Ec. The increase in β modifies the velocity distribution, weakening microrotation effects at the wall, while higher Ec reduces rotational gradients due to enhanced thermal energy. A similar decreasing trend in C_s is observed with increasing K and M. The increase in K enhances the spin-gradient viscosity, which redistributes microrotation effects away from the wall, whereas the magnetic field parameter M dampens both linear and angular motion, thereby reducing the couple stress at the surface.

Table 2: Values of skin friction coefficients, Nusselt number, and wall couple stress for $K, \alpha, \beta, \lambda, M$, and Ec.

K	α	β	λ	M	Ec	$f''(0)$	$-\theta'(0)$	$g'(0)$
1.0	1.0	0.5	1.0	0.2	0.5	0.356872	-0.258650	0.053320
2.0						0.331642	-0.298406	0.046323
5.0						0.294444	-0.380315	0.036895
1.0	0.2					0.380295	-0.077656	0.060729
	1.5					0.396542	-0.344141	0.064887
	2.0					0.406507	-0.516923	0.067497
	1.0	0.6				0.433712	-0.082993	0.064710
		0.8				0.551954	0.127600	0.072354
		1.0				0.700248	0.285081	0.084553
		0.5	1.5			0.367457	0.058590	-0.045074
			2.5			0.343642	0.053729	0.148114
			3.5			0.329873	0.050821	0.266159
				1.0		0.389147	-0.220357	0.062978
				1.5		0.405095	-0.211113	0.068359
				2.0		0.420679	-0.202868	0.073676
			1.0	0.2	0.3	0.356872	0.215578	0.053320
					0.7	0.331642	0.022363	0.046323
					1.0	0.294444	-0.293998	0.036895

Figures 2–4 illustrate the effects of the material parameter Kon the the velocity, microrotation, and temperature profiles across the boundary layer. Figure 2 shows that there is a decrease in the fluid velocity as well as in the hydrodynamic boundary layer thickness as K increases. Similarly, the microrotation distribution across the boundary layer reduces as K rises, with the negative values of the microrotation implying reverse spinning of the micro-particles, as shown in Figure 3. On the other hand, the temperature increases and the thermal boundary layer thickens with a rise in the material parameter K as depicted in Figure 4.

The micropolar heat conduction parameter α raises the thermal profile as observed in Figure 5. The profile of temperature distribution versus λ, the micropolar heat conduction coefficient, is displayed in Figure 6. It is noted from this figure that the heat profile decreases with a rise in λ. This is because heat is conducted away from the surface with a rise in this parameter. It shows that there is a cooling effect as λ is raised due to the contraction of the thermal boundary layer. In Figure 7, however, the velocity profile appreciates with higher values of β, the velocity ratio parameter. The micropolar fluid flow becomes accelerated with increasing values of β.

Figures 8 and 9, respectively, illustrate the impact of β on the heat and microrotation profiles. Observation shows that a rise in β causes a decreasing trend in $\theta(\eta)$, the thermal field. In the same manner, the microrotation field also falls as β grows in magnitude. There is a shrinkage in the heat boundary layer, and a cooling effect is exhibited due to a hike in the velocity ratio parameter. In a like manner, the microrotation boundary layer contracts as β amplifies.

Figures 10 and 11 illustrate the influence of the thermal radiation parameter (R) and Eckert number (Ec) on the temperature distribution. It is observed that both parameters significantly enhance the thermal field. Physically, an increase in (R) represents stronger radiative heat transfer within the fluid. This acts as an additional internal heat source, elevating the energy transport rate and effectively increasing the thermal diffusivity. Consequently, more heat penetrates the fluid, leading to higher temperatures and a thicker thermal boundary layer. Similarly, higher values of (Ec) indicate stronger viscous dissipation, where kinetic energy of the flow is converted into internal thermal energy due to fluid friction. This conversion becomes prominent in high-velocity or high-shear flows, resulting in a noticeable rise in fluid temperature. From an engineering perspective, these effects are particularly relevant in high-temperature systems such as thermal power plants, nuclear reactor cooling, metallurgical processing, and aerospace thermal protection systems, where radiative heat transfer and viscous heating play critical roles. In such applications, careful control of (R) and (Ec) is essential to prevent overheating, enhance thermal efficiency, and ensure system reliability.

Figures 12 and 13 illustrate the effect of the thermal conductivity parameter θ_R, and the Prandtl number Pr. Clearly, an increase in θ_R causes a rise in the temperature profiles and the thickening of the thermal boundary layer, as depicted in this picture. On the other hand, Figure 13 shows the effect of Prandtl number Pr on the temperature distribution across the boundary layer. Evidently, an increase in the magnitude of the Prandtl number causes a dampening effect on the temperature profiles and reduces the thermal boundary layer thickness. Thus, increasing Pr implies reducing the thermal boundary layer thickness, which in turn lowers the average temperature within the boundary layer. Increasing the Prandtl parameter can therefore be applied to enhance the rate of cooling in various heat transfer devices. Fluids with moderate Prandtl number create higher conductivities, and such heat diffuses more quickly away from the heated plate than for higher values of Pr.

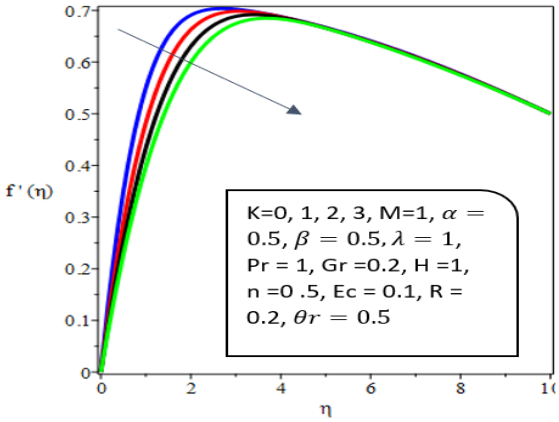

Figure 2: Effect of K on velocity profiles.

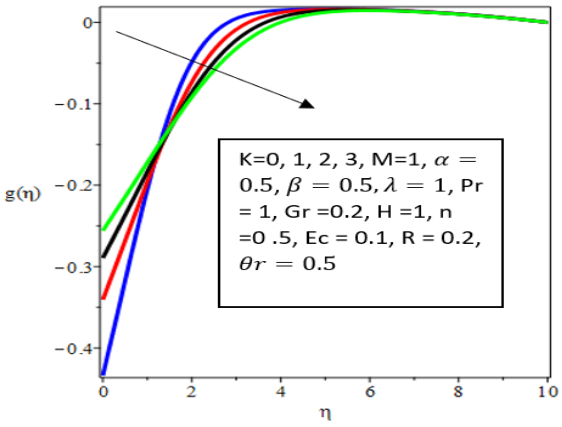

Figure 3: Microrotation profile for varying K.

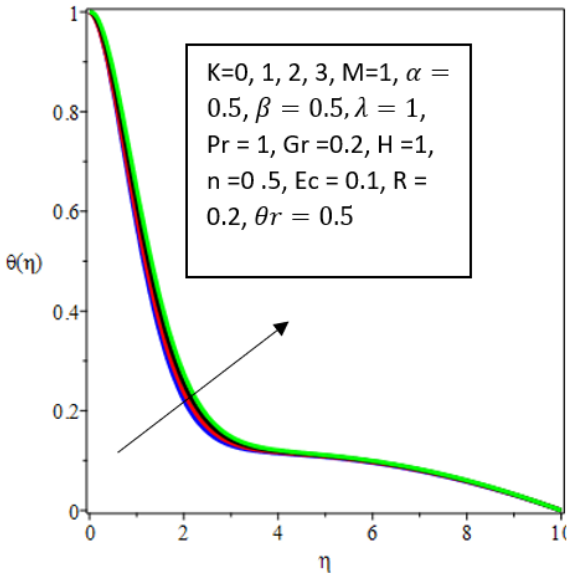

Figure 4: Effect of K on temperature profiles.

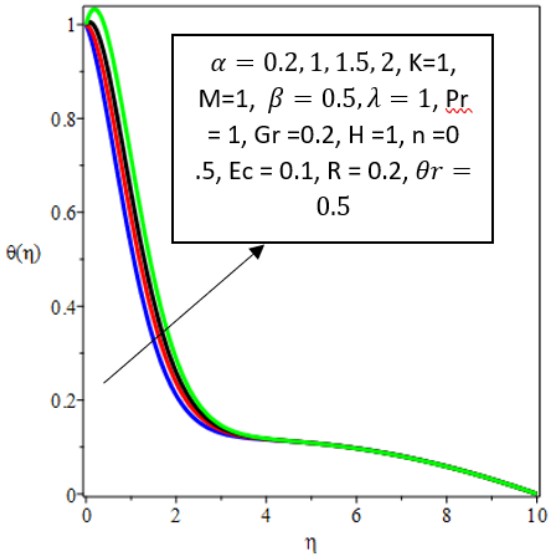

Figure 5: Temperature profile for varying α.

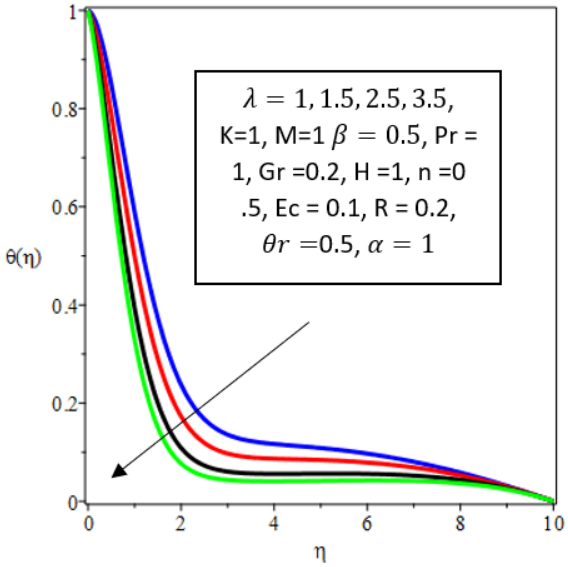

Figure 6: Effect of λ on velocity profiles.

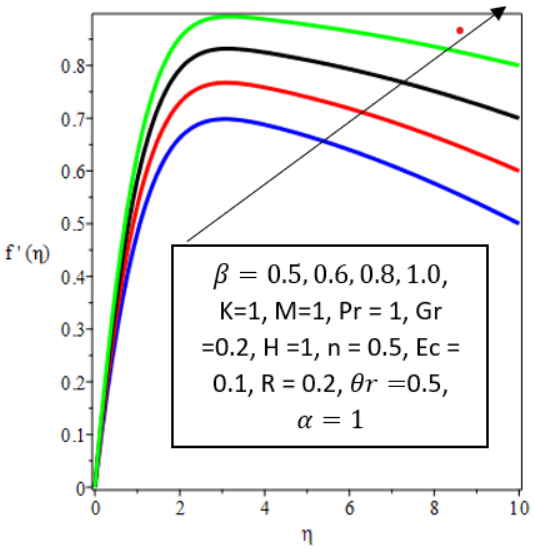

Figure 7: Temperature profile for varying β.

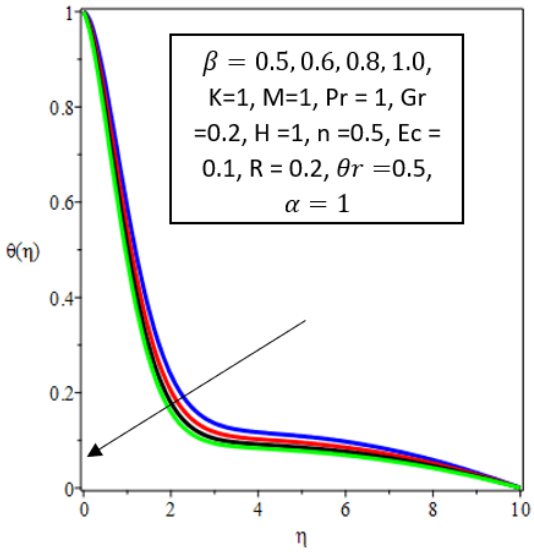

Figure 8: Effect of β on temperature profiles.

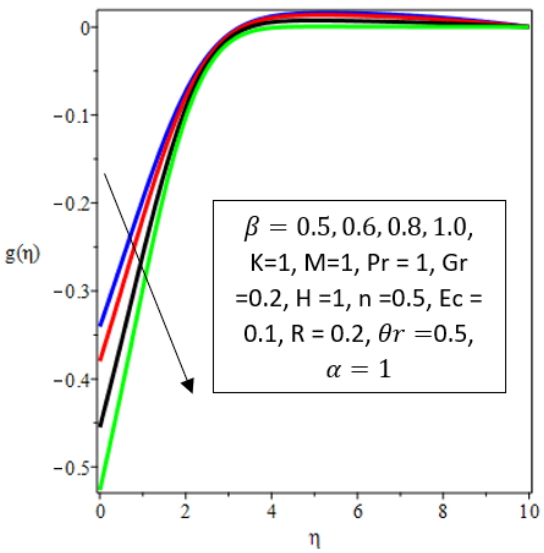

Figure 9: Microrotation profile for varying β.

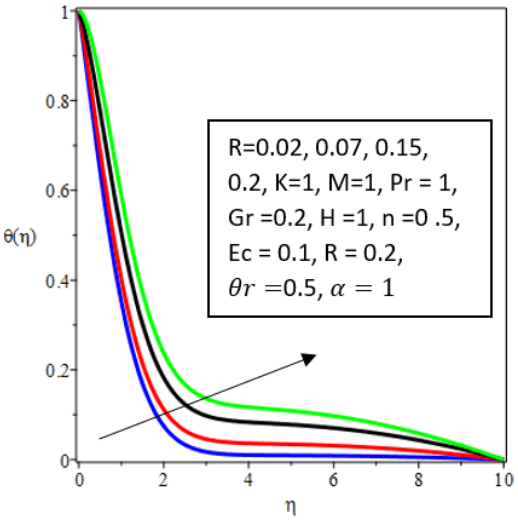

Figure 10: Effect of R on temperature profiles.

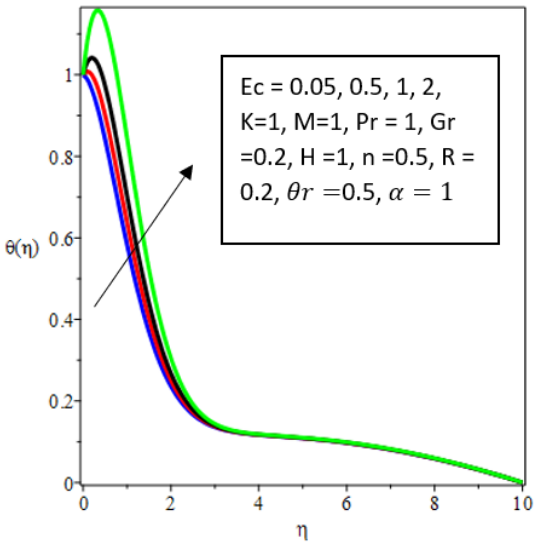

Figure 11: Thermal profiles for varying Ec.

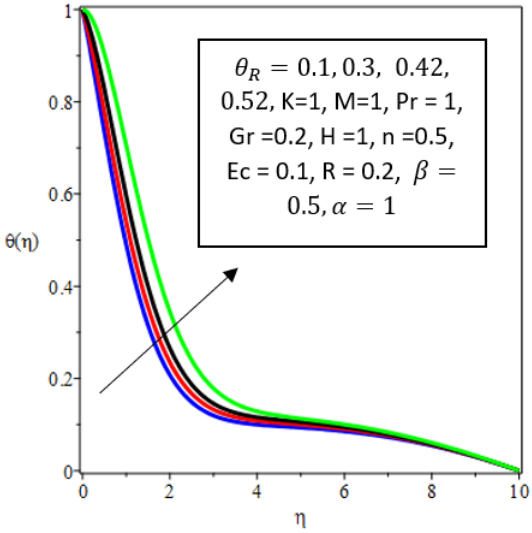

Figure 12: Effect of θ_R on temperature profiles.

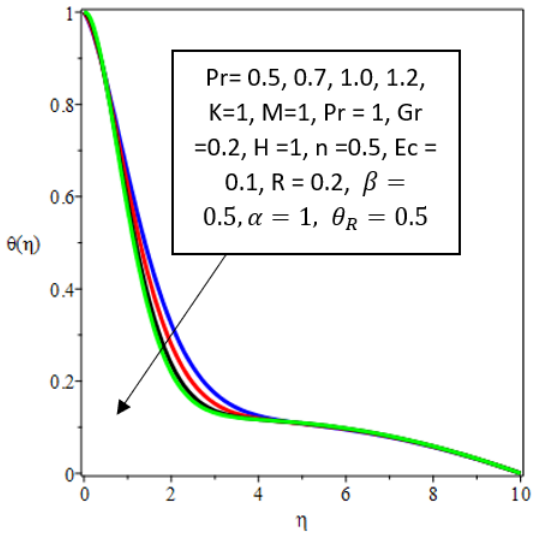

Figure 13: Effect of Pr on temperature.

5. Conclusion

The current study examines the flow dynamics and heat transfer phenomenon of thermally radiating MHD micropolar fluids under the influence of micropolar heat conduction along a vertical plate. The governing nonlinear equations were transformed and solved numerically to analyze the influence of key physical parameters on velocity, microrotation, and temperature distributions. The obtained results compare favourably with existing previously published results in the literature under some limiting scenarios. The results show that the micropolar material parameter K is capable of reducing both the velocity and microrotation profiles, and the viscous drag over the plane surface. It is an indication that enhanced microstructural resistance and reverse particle rotation are achievable by MHD micropolar fluid while simultaneously increasing the temperature field and thickening the thermal boundary layer.

The study clearly reveals that the interplay of viscous dissipation, micropolar heat conduction, magnetic field, and thermal radiation plays a crucial role in regulating transport phenomena. The results of which are valuable for the design and optimization of advanced thermal systems involving MHD micropolar fluids in engineering and energy applications. Other important results from the study are that:

A rise in the micropolar heat conduction parameter lowers the temperature distribution, enhancing heat diffusion away from the surface and producing a cooling effect.

Increasing the magnitude of the velocity ratio parameter causes the fluid motion to accelerate but reduces both temperature and microrotation profiles, leading to thinner thermal and microrotation boundary layers.

The velocity profiles decrease by elevating the values of the magnetic parameter due to the imposition of the Lorentz force, while increasing the temperature through Joule heating effects.

The thermal boundary structure expands by raising the magnitude of the radiation parameter, and as such, the temperature distribution enhances because this term introduces additional radiative heat flux in the boundary layer.

The temperature profiles are affected by the action of both thermal radiation and viscous dissipation because the two terms act as energy sources within the flow, leading to elevated temperature fields and thicker thermal boundary layers.

6. Suggestions for Further Studies

For the present study, several extensions can be considered for future investigation. The current model may be extended to unsteady flow conditions to capture transient thermal behaviour. The inclusion of variable thermophysical properties, nanoparticle aggregation effects, and non-Newtonian base fluids could further enhance the realism of the model. Additionally, the influence of the induced magnetic field at higher magnetic Reynolds numbers may be examined. Future studies may also explore different geometries, such as stretching/shrinking surfaces or porous media, as well as employ advanced numerical or analytical techniques to improve solution accuracy. Experimental validation of the present results would also be valuable for practical implementation in engineering systems.

Acknowledgments

The author appreciates the constructive comments of the anonymous reviewers, which helped improve the quality of this manuscript

Funding

The author received no external funding and personally supported this research

Competing Interest

The author affirms that there are no identifiable conflicts of interest, either financial or personal, that could be perceived as influencing the work presented in this paper.

Data Availability Statement

All data generated or analyzed during this study are included in this published article

Ethics Approval

This study is theoretical and numerical; therefore, ethics approval was not required

References

Abbas, N., Nadeem, S., & Khan, M. N. (2022). Numerical analysis of unsteady magnetized micropolar fluid flow over a curved surface. Journal of Thermal Analysis and Calorimetry, 147(11), 6449-6459.

Ahmadi, G. (1976). Self-similar solution of incompressible micropolar boundary layer flow over a semi-infinite plate, Int. J. Engng Sci, 14, 639-646.

Anantha Kumar, K., Sugunamma, V., & Sandeep, N. (2020). Influence of viscous dissipation on MHD flow of micropolar fluid over a slendering stretching surface with modified heat flux model: K. Anantha Kumar et al. Journal of Thermal Analysis and Calorimetry, 139(6), 3661-3674.

Arifuzzaman, S. M., Mehedi, M. F. U., Al-Mamun, A., Biswas, P., Islam, M. R., & Khan, M. S. (2018). Magnetohydrodynamic micropolar fluid flow in presence of nanoparticles through porous plate: A numerical study. International Journal of Heat and Technology, 36(3), 936-948.

Bejawada, S. G., & Nandeppanavar, M. M. (2023). Effect of thermal radiation on magnetohydrodynamics heat transfer micropolar fluid flow over a vertical moving porous plate. Experimental and computational multiphase flow, 5(2), 149-158.

Cortell, R. (2005). Flow and heat transfer of a fluid through a porous medium over a stretching surface with internal heat generation/absorption and suction/blowing, Fluid Dynamics Research 37 (2005) 231–245.

Fatunmbi, E. O. and Okoya, S. S. (2020). Heat Transfer in Boundary Layer Magneto-Micropolar Fluids with Temperature-Dependent Material Properties over a Stretching Sheet, Advances in Materials Science and Engineering, 2020, Article ID 5734979, 11 pages.

Fatunmbi, E. O., & Adeniyan, A. (2018). Heat and mass transfer in MHD micropolar fluid flow over a stretching sheet with velocity and thermal slip conditions. Open Journal of Fluid Dynamics, 8(2), 195-215.

Fatunmbi, E. O., & Salawu, S. O. (2020). Thermodynamic second law analysis of magneto-micropolar fluid flow past nonlinear porous media with non-uniform heat source. Propulsion and Power Research, 9(3), 281-288.

Fatunmbi, E. O., Obalalu, A. M., Khan, U., Hussain, S. M., & Muhammad, T. (2024). Model development and heat transfer characteristics in renewable energy systems conveying hybrid nanofluids subject to nonlinear thermal radiation. Multidiscipline Modeling in Materials and Structures, 20(6), 1328-1342.

Fatunmbi, E. O., Ogunseye, H. A., & Sibanda, P. (2020). Magnetohydrodynamic micropolar fluid flow in a porous medium with multiple slip conditions. International Communications in Heat and Mass Transfer, 115, 104577.

Garg, A., Akkinepally, B., Sarkar, J., & Pattanayek, S. K. (2025). Emerging perspectives in non-Newtonian fluid dynamics: Research gaps, evolving methods, and conceptual limitations. Physics of Fluids, 37(7), 071401.

Hayat, T., Khan, M. I., Waqas, M., Yasmeen, T., & Alsaedi, A. (2016). Viscous dissipation effect in flow of magneto-nanofluid with variable properties. Journal of Molecular Liquids, 222, 47-54.

Hsiao, K. L. (2017). Micropolar nanofluid flow with MHD and viscous dissipation effects towards a stretching sheet with multimedia feature. International Journal of Heat and Mass Transfer, 112, 983-990.

Jin, K., & Tian, Z. (2022). Effect of thermal radiation heat transfer on the temperature measurement by the thermocouple in premixed laminar flames. Journal of Thermal Science, 31(2), 541-551.

Kataria, H. R., Mistry, M., & Mittal, A. (2022). Influence of nonlinear radiation on MHD micropolar fluid flow with viscous dissipation. Heat Transfer, 51(2), 1449-1467.

Khan, M. N., Nadeem, S., & Muhammad, N. (2020). Micropolar fluid flow with temperature-dependent transport properties. Heat Transfer, 49(4), 2375-2389.

Kocić, M., Stamenković, Ž., Petrović, J., & Bogdanović-Jovanović, J. (2023). MHD micropolar fluid flow in porous media. Advances in Mechanical Engineering, 15(6).

Li, H., Wang, M., You, R., & Tao, Z. (2023). Impact of thermal radiation on turbine blades with film cooling structures. Applied Thermal Engineering, 221, 119832.

Pasha, P., Mirzaei, S., & Zarinfar, M. (2022). Application of numerical methods in micropolar fluid flow and heat transfer in permeable plates. Alexandria Engineering Journal, 61(4), 2663-2672.

Saleem, S., Nadeem, S., Rashidi, M. M., & Raju, C. S. K. (2019). An optimal analysis of radiated nanomaterial flow with viscous dissipation and heat source. Microsystem Technologies, 25(2), 683-689.

Sharma, S., Dadheech, A., Parmar, A., Arora, J., Al-Mdallal, Q., & Saranya, S. (2023). MHD micro polar fluid flow over a stretching surface with melting and slip effect. Scientific reports, 13(1), 10715.

Takhar, H. S., Nath, G. & Gupta, R. K. (1998). Unsteady flow and heat transfer on a semi-infinite flat plate with an aligned magnetic field, International Journal of Engineering Science, 36, 1781–1797.

Wu, W. T., & Massoudi, M. (2020). Recent advances in mechanics of non-Newtonian fluids. Fluids, 5(1), 10.

How to Cite: Adeniyan, A. & Fatunmbi, E.O. (2026). Effects of viscous dissipation and micropolar heat conduction on thermally radiating MHD flow along a vertical plate. *Science Research Annals–Physical Sciences,* 2(1), 13–21. https://doi.org/10.63112/zys4jd37